We are IntechOpen, the world's leading publisher of Open Access books Built by scientists, for scientists

6,900
Open access books available

185,000
International authors and editors

200M
Downloads

154
Countries delivered to

Our authors are among the

TOP 1%
most cited scientists

12.2%
Contributors from top 500 universities

CLARIVATE ANALYTICS
BOOK CITATION INDEX
INDEXED

WEB OF SCIENCE™

Selection of our books indexed in the Book Citation Index
in Web of Science™ Core Collection (BKCI)

Interested in publishing with us?
Contact book.department@intechopen.com

Numbers displayed above are based on latest data collected.
For more information visit www.intechopen.com

Photoluminescence Studies on ZnO Thin Films Obtained by Sol-Gel Method

Guadalupe Valverde Aguilar,
Mónica R. Jaime Fonseca,
Ángeles Mantilla Ramírez and
Antonio G. Juárez Gracia

Additional information is available at the end of the chapter

Abstract

The sol-gel process is a friendly room temperature method to prepare transparent glasses in the form of monoliths, films, and fibers. The zinc oxide films have been obtained by sol-gel method, which are very important materials in the ceramic technology due to their piezoelectric properties and applications in various pressure transducers and acoustic-optic devices, surface and bulk acoustic wave devices, and solar cells. Structure and characteristic ultraviolet-blue emissions of amorphous and crystalline zinc oxide thin films–coated glass substrates by dip-coating deposition are explained by photoluminescence studies in this chapter.

Keywords: sol-gel, thin film, zinc oxide, photoluminescence

1. Introduction

Sol-gel method is a very attractive chemical route due to its simplicity and flexibility in the use of different source materials that allow to synthesize amorphous and polycrystalline materials at low cost. The focus of this chapter is to expand on that knowledge about this method as an efficient route to obtain amorphous and crystalline ZnO thin films particularly. It is well known that the ZnO thin films are very important materials in ceramic technology and thin films technology due to numerous properties, while the ZnO nanocrystals with high stability at low processing temperatures have applications in displays, emitters, and sensors. The optical properties of excitons confined in the ZnO nanocrystals were studied by optical

absorption, infrared spectroscopy and photoluminescence studies. The photoluminescence mechanisms of the violet and blue emissions are discussed in detail.

2. Sol-gel process

Materials prepared by the sol-gel process have become the source of an important field of research in materials science since the 1970s. The sol-gel process is a room temperature method of preparing transparent inorganic glasses without melting [1, 2], which is much lower compared to the high temperatures needed by standard glass manufacturing processes. The fabrication of glasses or ceramic materials involves a set of reactions such as hydrolysis and condensation that convert an aqueous metal alkoxides [2] with a molecular formula of $M(OR)_n$ into different types of inorganic networks. The advantage of this process has the advantage of being able to yield high purity inorganic oxide glasses, besides versatile in creating different types of materials (thin films, spun fibers, particles, aerogels, and xerogels).

As the name implies, the sol-gel process is the conversion of a sol to a gel. The sol-gel process is therefore a series of hydrolysis and condensation reactions of the inorganic alkoxide monomers that forms colloidal particles (sol) and converts them into a continuous network (gel). Usually for the preparation of silicate materials, tetramethoxysilane (TMOS) or tetraethyl orthosilicate (TEOS) is the most popular alkoxides. TEOS can be hydrolyzed and condensed under relatively mild conditions to manufacture silica gels. The hydrolysis step of TEOS can be represented as the Equation: $Si(OEt)_4 + H_2O \rightarrow HO\text{-}Si(OEt)_3 + EtOH$. The first step in this equation is the generation of a silanol group (Si-OH) and the corresponding alcohol. The second step is the condensation of the silanol group. This step can occur in two different ways and is represented by the equation $HO\text{-}Si(OEt)_3 + HO\text{-}Si(OEt)_3 \rightarrow (EtO)_3\text{-}Si\text{-}O\text{-}Si(OEt)_3 + H_2O$ and $HO\text{-}Si(OEt)_3 + Si(OEt)_4 \rightarrow (EtO)_3\text{-}Si\text{-}O\text{-}Si(OEt)_3 + EtOH$.

The process continues as the silanol groups condense with other silonols groups or with an alkoxide. If the silonols condense with an alkoxide, they make siloxane bonds (Si-O-Si) that have water or an alcohol as a byproduct. By repeating these steps many times, a gel or a solid material is generated. The hydrolysis reaction can be greatly influenced by the presence of an acid or a base. Conducted in the presence of an acid catalyst, the hydrolysis step involves the electrophilic attack from the proton on the alkoxide oxygen atom resulting oxygen having a positive charge. This leads the bond between the silicon center and the oxygen that was attacked to become more polarized and facilitates the departure of the alcohol to form the silanol bond. In the case of a base catalyzed reaction, the hydroxyl attacks the silicon atom, and the alcohol group leaves to form $HO\text{-}Si(OEt)_3$. The hydrolysis reaction is much faster under acidic condition than under basic.

The pH of the solution also affects the condensation rates of the reaction which happens in two steps. The first step is the electrophilic attack of the proton on the oxygen of the silanol group. The second step is the formation of the siloxane bond after the loss of the hydronium cation. Similarly under basic conditions, the condensation reaction also has two steps. The hydrogen on the silanol group gets deprotonated by the hydroxide ion leaving a

negatively charged oxygen on the silanol. This results in the formation of the siloxane bonds. The condensation rate under basic conditions is faster than that under acidic conditions.

Because the hydrolysis and condensation rates differ depending on the catalyst used, the structures can also be controlled by using the right catalyst. For acid catalysis, the hydrolysis reaction is faster than the condensation reaction. As a consequence, a network with less siloxane bonds and more silanol groups yields more linearly branched polymeric species. This makes this catalyst the preferred method for the formation of thin films. On the other hand, the condensation reaction is much faster using base as a catalyst. Therefore, there are fewer silanol groups in the network. The network then consists of highly branched clusters, which yields denser materials. This is the method used for the formation of particles.

The typical mixture involves TMOS or TEOS, water, a solvent as methanol or ethanol followed by the addition of a catalyst (hydrochloric acid, for example). During the sol-gel formation, the viscosity of the solution gradually increases as the sol, which is a colloidal suspension of small particles with sizes about 1–100 nm that are well dispersed in a liquid. It becomes interconnected through polycondensation reactions to form a rigid, porous network that contains a phase of continuous liquid, the gel. The gelation stage will take place depending of the conditions as Si:H_2O ratio, type and concentration of catalyst, alkoxide precursors, etc. This stage can spend from seconds to minutes, or days to months. In the final stage, drying, the alcohol and water evaporation from the pores produces the gel shrinks.

The advantages of using the sol-gel process are (1) the method is performed at room temperature so molecules that could easily denature at higher temperatures can be added to the glasses [3], (2) it allows the easy fabrication of the materials in various configurations such as monoliths, powders, fibers, and films (**Figure 1**), (3) the material is transparent so spectroscopic studies can be used to probe the chemistry going on in the material, (4) the chemical properties of the sol-gel-derived oxides can be manipulated by incorporating organic, organometallic, and inorganic functional groups into the gel framework [4], (5) the materials are chemically, photochemically, and electrochemically stable, and (6) the matrix can stabilize the entrapped reagent from photodegradation, oxidation process, or not friendly environments.
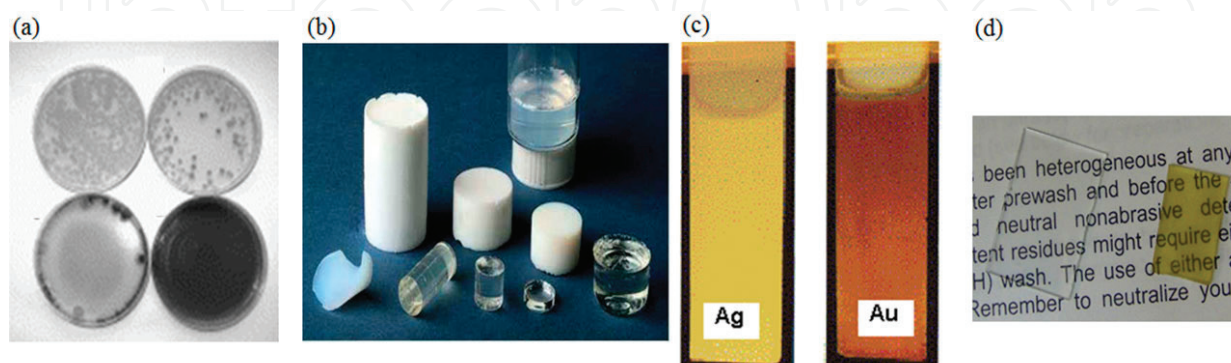

Figure 1. Picture of (a) monoliths doped with different concentrations of Ag, (b) monoliths of silica, TiO_2 and ZnO, (c) sol-gel films silica dip-coated onto glass wafers containing metallic nanoparticles, and (d) sol-gel films titania spin-coated onto glass wafers containing silver and iron nanoparticles.

Thin films are utilized as chemical sensors applications due to the short path length for diffusion. Bulk monoliths are often used for spectroscopic measurements due to their longer optical path length, while the powders are used in catalysis applications due to their high surface area.

As mentioned before, sol-gels can be made into powders, monoliths, films, and fibers. Monoliths can be prepared by casting the sol into a mold of any size or shape. The monolith undergoes gelation, aging, and drying to form the final xerogel. Films can be made by either spin coating [5] or dip coating [6] the sol onto a substrate, see **Figure 2**. Spin coating is a technique used since the 90s used to deposit thin films on different types of flat substrates. Placed a drop of liquid or semi-liquid precursor solution centered on the substrate (glass, silicon, etc.), which rotates at a high speed, around 3000 or 4000 rpm causing that the fluid is spread by the action of the centripetal acceleration. The thickness and properties of the final film depend on the precursor solution (viscosity, concentration, surface tension, etc.), as well as the spin-coater parameters as the rotational speed, time, and revolutions per minute (rpm). Any variation in the values of these parameters can alter the thickness and properties of the coated film. A precursor solution was placed on the glass wafers (2.5×2.5 cm^2) using a dropper and spun at a rate of 4000 rpm for 15 s, for example.

The technique of spin coating is widely used in the photolithography, in the manufacture of films with thicknesses lower than 10 nm, and to deposit photoresistances of near a micrometer wide.

Amorphous and crystalline ZnO thin films can be produced via a combined sol-gel route with spin-coating technique. First, a ZnO precursor solution can be prepared by sol-gel process. Then, this solution can be deposited on glass and silicon wafers by spin-coating technique to obtain amorphous thin films. Crystalline films are obtained by calcination process between 450 and 550°C to produce ZnO nanocrystals into the films [7].
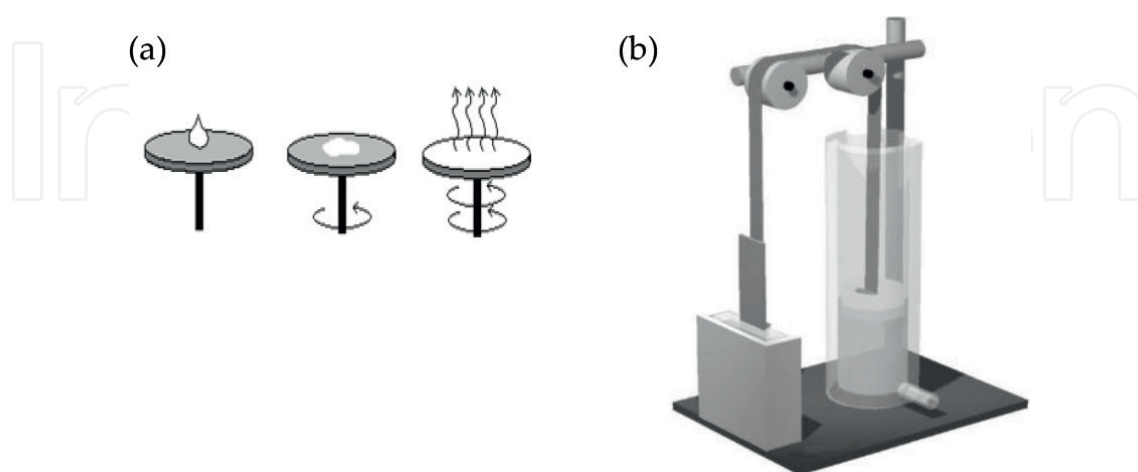
Figure 2. (a) Spin-coating technique [5] and (b) dip-coater device [6], both used to deposit sol-gel thin films on to silicon or glass substrates.

3. Photoluminescence

Luminescence is the process of emission of light by atoms or molecules excited. There are three types of luminescence procedures: *molecular fluorescence*, *phosphorescence*, and *chemiluminescence*. In these procedures, the molecules of the analyte are excited to give species whose emission spectrum provides information for qualitative or quantitative analysis.

A molecule in the ground state is raised to the excited state due to the absorption of photons that have enough energy. The excited molecules undergo a vibrational relaxation of the level of energy toward the lowest excited state by nonradiative processes and then return to ground state by emitting photons. The phenomena of fluorescence and phosphorescence fall within this definition, and therefore, the two phenomena are often referred by the general term *photoluminescence*. The fluorescence differs from phosphorescence by the electronic energy transitions which do not imply a change in electron spin. In terms of decay, the fluorescence is a radiative decay of the singlet state to the ground state occurring almost immediately, in about 1 ns. On the contrary, the time of half-life of triplet states is very large. This is why its decay to the ground state results in phosphorescence produced via one photon, since it can also decay by nonradiative processes. The chemiluminescence is based upon the emission spectrum of an excited species that is formed during a chemical reaction. Sometimes, the excited particles are produced by this reaction between the analyte and a suitable reagent (as a strong oxidant such as ozone or hydrogen peroxide), and a spectrum characteristic of the oxidation product of the analyte is observed instead of the analyte itself.

The main features of the luminescence methods are the sensitivity and selectivity. The luminescence tends to be three orders of magnitude smaller than those encountered in absorption. The selectivity of the luminescent is usually higher than that for absorption. There are many species capable of absorbing radiation, but the number of them that can reemit is much smaller; besides the excitation wavelength, as the emission can be selected to minimize interferences, while in spectrophotometry, only the wavelength of absorption is selectable.

Other advantage of photoluminescence method is their large linear concentration ranges, which are often significantly greater than those encountered in absorption methods. Finally, the selectivity of luminescence procedure is often better than that of absorption methods.

Luminescent materials have been used for more than a century for ionizing radiation detection, and the search for new and more efficient detector materials has been intense. Currently, a new promising direction of this research has emerged as the luminescence of nanocrystals. The basis for this is the observed luminescence intensity dependence on nanocrystal size [8]. The observed greater luminescence intensity for smaller size nanocrystals is explained by enhanced oscillator strength of the excitons [9].

3.1. Singlet/triplet excited states

A molecular electronic state in which all electrons spins are paired is called a *singlet* state, and no splitting of energy level occurs when the molecule is exposed to a magnetic field

(the effects of the nuclear spin are negligible). On the other hand, the ground state for a free radical is a *doublet* state since the odd electron has two orientations in a magnetic field, resulting slightly different energies to the system.

A singlet or a *triplet* state is allowed if one of a pair of electrons of a molecule is excited to a higher energy level. In the excited single state, the spin of the promoted electron is still paired with the electron that is the ground state, while, in the triplet state, the spins of both electrons disappear. **Figure 3** shows a representation of both states.

3.2. Energy level diagrams for photoluminescent molecules

Figure 4 shows a partial energy level diagram for a typical photoluminescent molecule. The lowest heavy horizontal line represents the ground state energy of the molecule, which is a single state labeled as S_0. At room temperature, this state represents the energies of essentially all of the molecules in a solution.

The heavy lines above are energy levels for the ground vibrational states of three excited electronic states. The two lines on the left represent the first (S_1) and second (S_2) electronic singlet states. The one on the right (T_1) represents the energy of the first electronic triplet state. As usually happens, the energy of the first excited triplet state is lower than the energy of the corresponding singlet state. Several vibrational energy levels are associated with each of the four electronic states, as suggested by the lighter horizontal lines.

The excitation of this molecule can be brought about by absorption of two bands of radiation, one centered about the wavelength λ_1 ($S_0 \rightarrow S_1$) and the second around the shorter wavelength λ_2 ($S_0 \rightarrow S_2$). The direct excitation to the triplet state is not shown. This transition does not occur to any significant extent, because this process involves a change in multiplicity, and even that, it has a low probability of occurrence, it is called a forbidden transition.
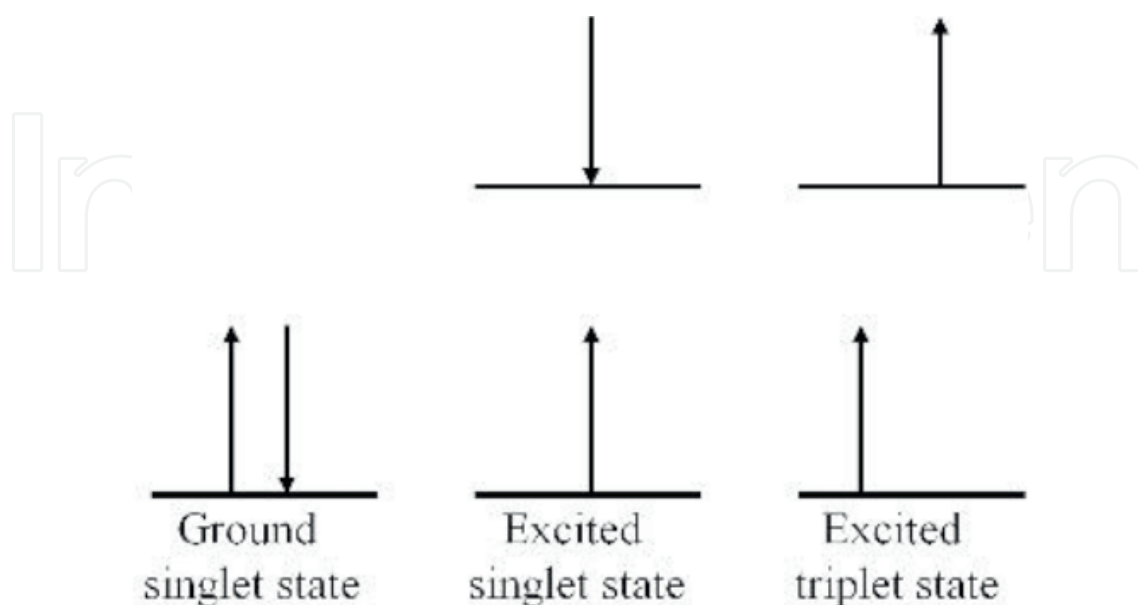
Figure 3. Schematic representation of different molecular electronic states.
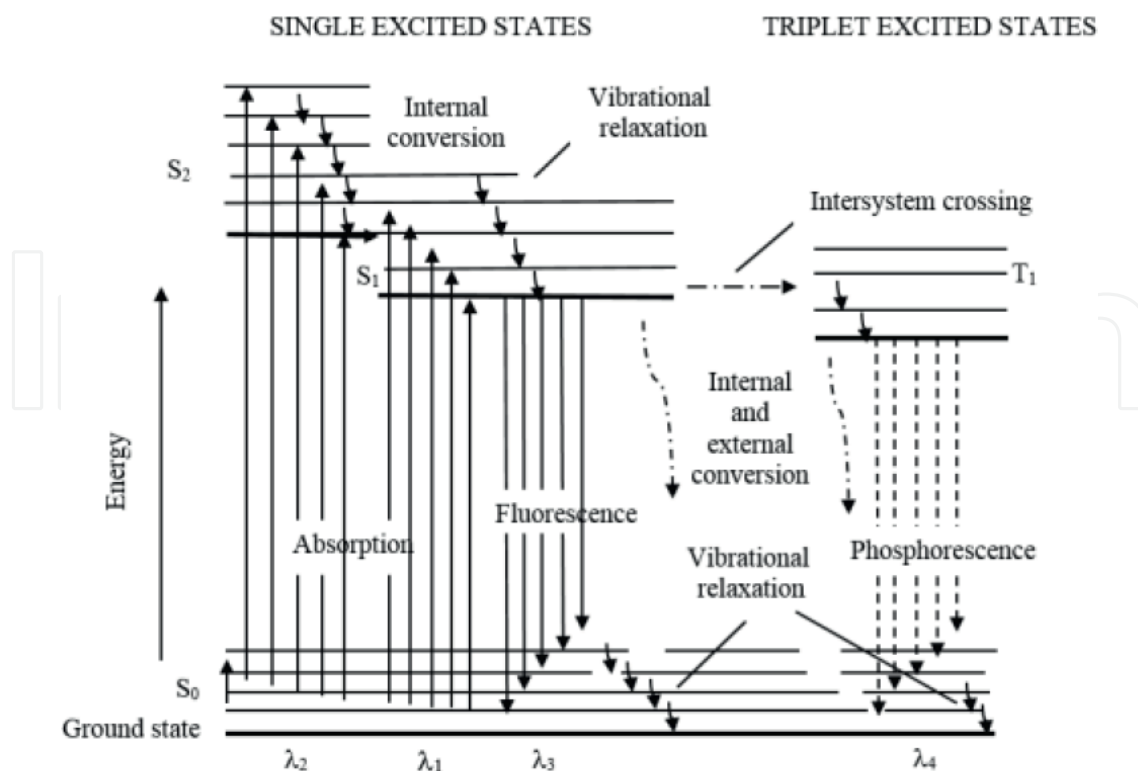
Figure 4. Partial energy diagram for a photoluminescent system.

The luminescent material ZnO exhibits two groups of luminescence bands: (i) in the region 1.8–2.4 eV due to defects and (ii) in the region 3.1–3.3 eV due to excitons [10]. The exciton luminescence lifetime is below 1 ns in ZnO [11], and therefore, it is possible to obtain a very fast scintillator. Luminescence of ZnO has been studied for thin films [12, 13], nanocrystals suspended in propanol [14], and nanocrystals embedded in solid matrices [15].

The luminescence can be influenced by the interface layer between a nanocrystal and the matrix [16]. ZnO nanocrystals (i.e., not embedded in any matrix) can modify the surface and luminescent properties.

4. Zinc oxide

Table 1 contains the main properties of the Zinc oxide (ZnO) [17–21], which is a semiconductor with a direct band gap of 3.37 eV at room temperature, and has a very stable even at room temperature which guarantee more efficient exciton emission at higher temperatures. The ionicity of this semiconductor resides at the borderline between covalent and ionic semiconductors. The difference of the electronegativities between the zinc and oxygen produces a high degree of ionicity in the bond. This produces an intense repulsion between the clouds of the charges from neighboring atoms with similar electrical loadings, making its crystalline structure more stable as hexagonal type, wurtzite. Due to its excellent chemical and thermal stability and specific optoelectronic properties, the ZnO has been used as

Property	Symbol (units)	Value
Lattice parameters	a, c, (Å)	3.253, 5.213
Coordination geometry	-	Tetrahedral
Fusion temperature	T_f (K)	>2250
Melting point	°C	2000
Density	ρ (g·cm^{-3})	5.675
Refractive index	n_D	2.0041
Fractional ionic character	-	0.62
Std enthalpy of formation	ΔH (Jmol^{-1})	6.5×10^3
Std entropy of formation	ΔS (J·mol^{-1}·K^{-1})	100
Specific heat	C_p (J·mol^{-1}·K^{-1})	41
Thermal expansion coefficient	α_a (K^{-1}) α_o (K^{-1})	6.5×10^{-6} 3.0×10^{-6}
Thermal conductivity	λ (W·m^{-1}·K^{-1})	0.6
Elastic constants (300 K, 10 Gpa)	C_{11} (Pa) C_{12} (Pa) C_{13} (Pa) C_{33} (Pa) C_{55} (Pa) C_{66} (Pa)	20.70 11.77 10.61 20.95 4.48 0.45
Dielectric constants	$\varepsilon_{0||}, \varepsilon_0{}^{\perp}$ $\varepsilon_{\infty||}, \varepsilon_\infty{}^{\perp}$	8.75, 7.8 3.75, 3.70
Band gap (2 K) Band gap (300 K)	E_g (eV) E_g (eV)	3.42 3.35
Exciton binding energy	E_b (meV)	60
Effective mass of electrons	m_η	$0.28·m_0$
Effective mass of holes	m_ϱ	$0.58·m_0$

Table 1. Physical properties of ZnO.

photonic crystals, field emissions, photodetectors, photodiodes, light-emitting diodes, solar cells, varistors, gas sensors, and photocatalytic materials. Besides, the zinc oxide is a non-toxic material, it does not cause skin and eye irritation and there is no evidence of carcino-genicity, genotoxicity and reproduction toxicity in humans. There have been some concerns about the potential adverse effects on human health or the environment. Nevertheless, the current evidence shows that the ZnO particles or nanoparticles do not penetrate cells of the skin and remain on the outer layer of undamaged skin (the stratum corneum) with low systemic toxicity.

4.1. Technological applications

Zinc oxide has a wide variety of applications as luminescent material, such as vacuum fluorescent displays due to its room temperature ultraviolet emission and nonlinear optical properties. The combination of being a large-bandgap semiconductor and a luminescence material has allowed to study as nanostructured ZnO such as nanoparticles, nanowires, nanobelts, and nanotube [22]. Due to its crystalline structure, wurtzite, the ZnO has three exciton states called A, B, and C, whose energies are 3.3768 eV (367 nm), 3.3834 eV (366 nm), and 3.4223 eV (362 nm), respectively [21].

Specifically, the ZnO as thin film has relevant applications in ceramic technology and thin films technology [23–25]. ZnO nanocrystals with high stability at low processing temperatures have applications in displays, emitters, and sensors [23]. As films, exhibits a combination of piezoelectric, electrical, optical, and thermal properties, which have been already applied in devices as gas sensors, ultrasonic oscillators, and transparent electrodes in solar cells. Literature reports that pure and doped ZnO films have been produced by chemical vapor deposition, sputtering, spray pyrolysis, and the sol-gel process just to mention some methods of synthesis. At this point, our attention will be focus on the sol-gel route in combination with the dip-coating process to produce ZnO thin films, which represents an easy low cost and efficient route to coat large surfaces, permitting also the tailoring of the microstructure from the chemistry of the sol-gel synthesis [22, 24].

Special attention is deserved to the application as optoelectronic devices. On one hand, the fact of having the same crystal structure (with a difference of 2.0% and 0.5% for the parameters a and c, respectively) than the GaN [12], the material most studied so far for this application makes the ZnO an excellent substrate for heteroepitaxial growth. Its high exciton binding energy can permit the stimulated emission at temperatures higher than the environmental values (~550 K). All these properties have made that the study of ZnO has grown exponentially in recent years, especially after obtaining stimulated emission at room temperature in ZnO layers.

ZnO compounds doped with impurities are used as photoconductors in electrophotography, ceramic varistors, and sensor elements in the detection of combustible gases. As thin film, ZnO can exhibit piezoelectric properties, which can be used in pressure transducers and several acoustic-optical devices. ZnO doped with Al and I is used as transparent conductive electrodes to construct fluorescent screens because of their non-linear optical properties, and as solar cells made with ZnO, colloids show quantum size effects and luminescence. Furthermore, by it being ZnO oxide semiconductor material and the bandgap at room temperature, it becomes an emitter potential ultraviolet light at room temperature (such as ZnSe and GaN). Another important property of this material is the photocatalysis, which means that under illumination, this material can degrade organic pollutants, such as polluted water [25]. In this aspect, the ZnO shares this property with TiO_2 whose bandgap is 3.2 eV. But unlike the latter, the ZnO is not degraded by the photocorrosion. As gas sensor, it is known that ZnO is a good sensor of methanol, ethanol, propyl alcohol, LPG (Liquefied petroleum gas), carbon monoxide, and hydrogen.

The preparation as films has great advantages over other sensors. Since they can be manufactured in small sizes at large scale and at a lower cost, they are highly compatible with microelectronic and circuit technology, and additionally, incorporating impurities can give greater sensitivity ZnO film [22].

4.2. Crystal structure of ZnO: wurtzite

Under ambient conditions, the crystal structure of ZnO, wurtzite, is the most stable phase thermodynamically [26]. It has a hexagonal unit cell with two lattice parameters a and c, which ratio, and it is catalogue in the space group according to the Schöemflies notation and $P6_3mc$ in the Hermann-Mauguin notation. The parameters cell are a = b = 0, 381 nm and c = 0, 623 nm. Two hexagonal close-packed (hcp) sublattices interlace, each one consists of one type of atom displaced with respect to each other along the threefold c-axis by the amount of u = 3/8 = 0.375 in fractional coordinates. It consists of zinc and oxygen atoms tetrahedrally coordinated stacked according to the sequence ABABAB [27]. In such structure, the atoms are sufficiently far apart to compensate for the electrostatic repulsion. Each zinc atom is surrounded by a tetrahedron of four oxygen atoms and vice versa, which can be seen in **Figure 5**.

Lattice: Hexagonal

$a_1 = a(1,0,0)$

$a_2 = a(-1/2,3^{1/2}/2,0)$

$a_3 = c(0,0,1)$

Basis: 2 atoms

$\begin{cases} (0,0,0) \\ (a_1/3, a_2/3, a_3/2) \end{cases}$

Hexagonal Close-Packed structure

(HCP)

Wurtzite

Hexagonal lattice +

$(0,0,0)\ \left(a/2, a/2\sqrt{3}, c/2\right)$

first specie

$(0,0,0)\ \left(a/2, a/2\sqrt{3}, c/2 + cu\right)$
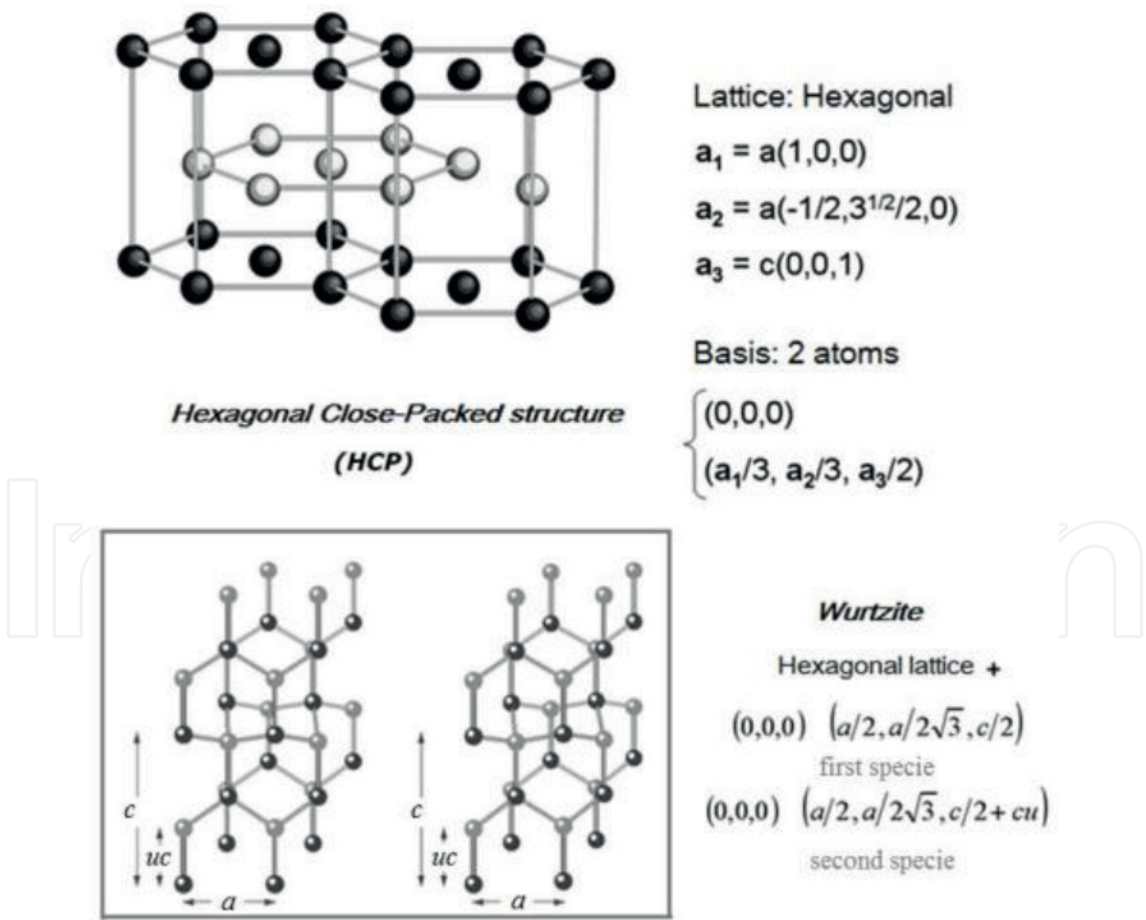
second specie

Figure 5. Structure of the primitive cell from ZnO. ● oxygen, ● zinc.

## 4.3. Optical properties of ZnO thin films

As mentioned above, the interest in ZnO has been motivated by possible optoelectronic applications. This is because it seems to be able to replace the compounds based on GaN that currently are used in optoelectronic devices as LEDs, laser diodes, and photodetectors that operate in the blue or UV range being cheaper and nontoxic. Other important factor that influences in this selection is the similarity of its band gap energy (3.37 eV at room temperature) with that of GaN (3.39 eV at room temperature) and the exciton binding energy of ZnO (60 meV) which is larger than that of GaN (18–28 meV). It can be useful in light-emitting devices. Emission properties of ZnO nanocrystals are influenced by many factors such as synthesis method, morphology of the crystals, dopants, and ligands used for surface coating.

4.3.1. Infrared spectra

Typical absorption spectra from amorphous and crystalline ZnO thin films taken at room temperature in the range of 300–900 nm are shown in **Figure 6**. The absorption spectrum of the amorphous film does not exhibit any band. After calcination process between 400 and 500°C [25, 26, 28], the spectrum of the crystalline film shows a narrow absorption peak A located around at 359 nm due to free excitons [21].

4.3.2. Optical absorption spectra

Other optical characterization on ZnO films is performance by infrared spectroscopy, shown in **Figure 7**. For amorphous and crystalline films, similar absorption bands were observed, and their respective assignment is described at **Table 2**. After the calcination treatment, the absorption bands located at 1342, 1410, 1557, 2900, 2945, and 3263 cm^{-1} disappeared.
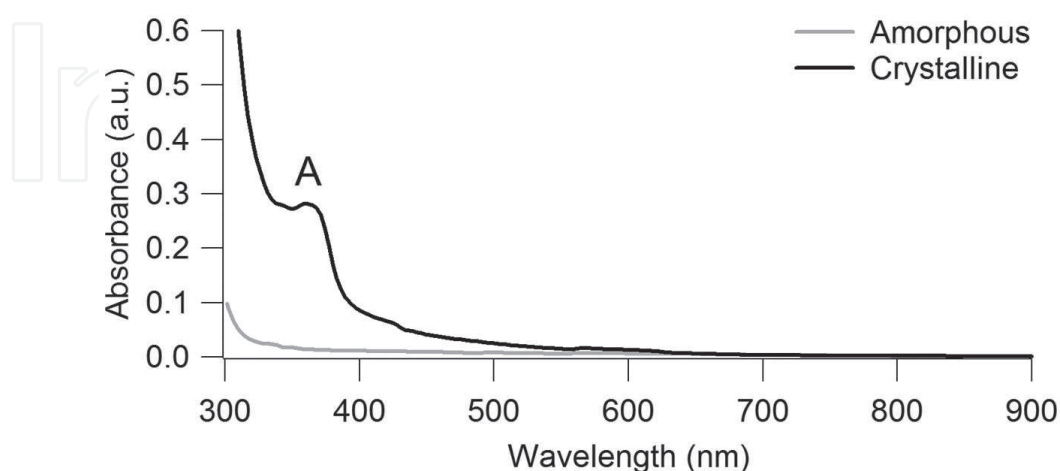
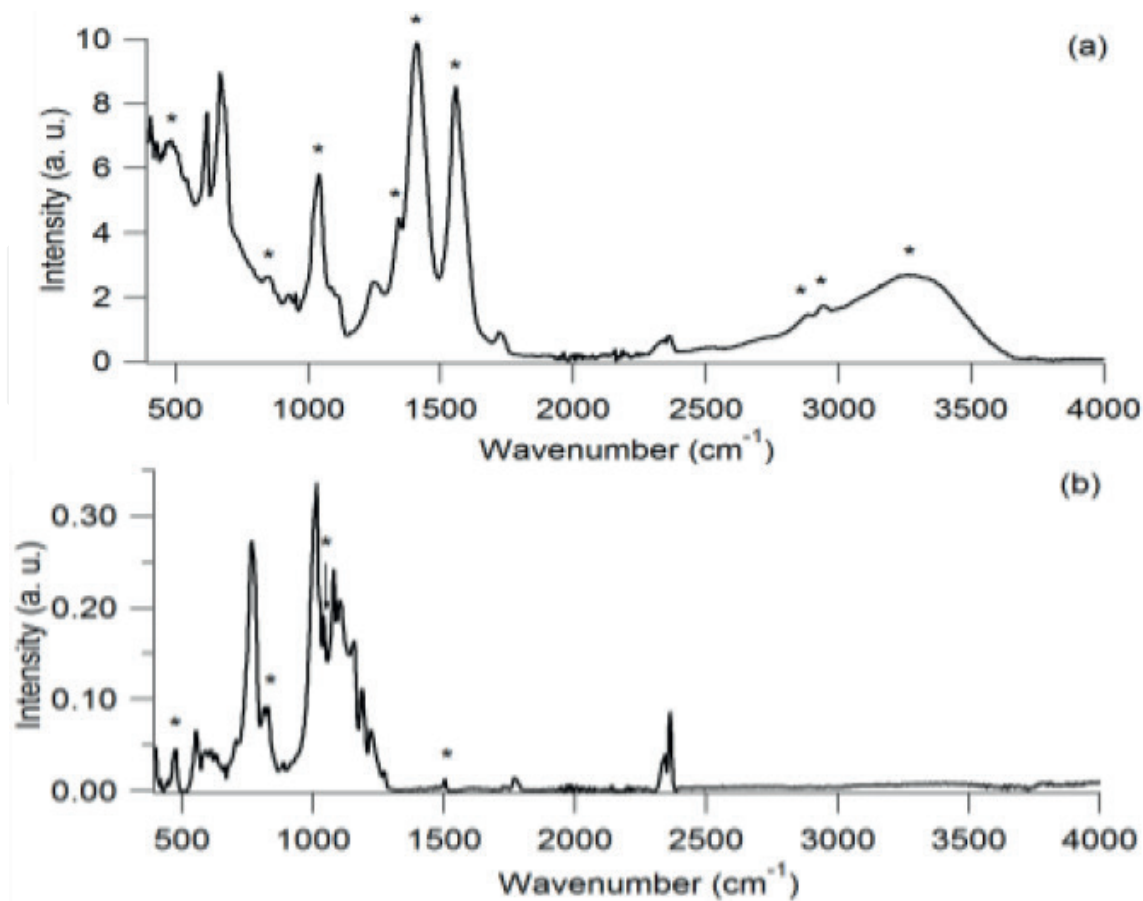**Figure 6.** Absorption spectra from amorphous ZnO film (gray line) and crystalline ZnO film (black line).

Figure 7. IR spectra of (a) amorphous ZnO film and (b) crystalline ZnO film.

ν_{exp} (cm^{-1}) Amorphous	ν_{exp} (cm^{-1}) Crystalline	Assignment	Ref.
478	476	ZnO stretching	[29]
854	842	Symm. bending ZnO	[29]
1042	1038	Asymm. stretching ZnO	[29]
1342	-	HOOC-R	[30]
1410	-	C-O	[31]
-	1502	Stretching mode of ZnO·H$_2$O	[29]
1557		C=O	[31]
2900	-	C-H stretching	[30]
2945	-	C-H stretching	[30]
3263	-	H-O species	[29]

Table 2. IR frequencies [in cm^{-1}], of the amorphous and crystalline ZnO films.

### 4.4. Photoluminescence studies on ZnO thin films

Photoluminescence studies have been performed on ZnO thin films by different emissions as near ultraviolet, red, green, and blue. However, the recombination centers and possible mechanisms to explain the mentioned emissions are not clear totally. A crucial factor is the fact that the luminescence of the ZnO is very sensitive to its surface state determined and modulated by the synthesis method. Also, the kind of substrate can influence the luminescence of the film ZnO deposited on it. Although these factors can lead to different optical phenomena, in general, all published works coincide in the assignment of the emission bands mentioned.

Particularly, the sol-gel method can be an appropriated route to maximize the luminescent properties of the ZnO films. Typical room temperature luminescence emission spectra of ZnO nanocrystals (crystalline film) synthesized by sol-gel method are shown in **Figure 8**. The luminescent response of these nanocrystals, the amorphous film, and the silicon wafer was compared. The excitation wavelength of ZnO was 359 nm, which coincides with the maximum absorption (**Figure 6**). The D and E bands located at 561 nm and 626 nm correspond only to the substrate, silicon wafer. Three main luminescent bands from ZnO were identified as A, B, and C. **Table 3** summarizes the maximum emission peaks for amorphous and crystalline ZnO films. Their luminescence behavior is identified with a small violet emission A band and a narrow blue emission B and C bands.

The visible emission of the ZnO films is related to different intrinsic defects, such as oxygen vacancies, zinc vacancies, zinc interstitials, oxygen interstitials, and anti-site defect O_{Zn} [32]. The luminescence emission characteristics of ZnO films are dependent on both the crystal quality of the film and the film stoichiometry [32].

From **Figure 8**, among the most notable differences is the shape of all bands, which is more defined from crystalline film than amorphous film. The intensity of the photoluminescent peak arises for crystalline film in comparison to the amorphous one [33]. The crystallization of the ZnO film increases the visible emissions due to the increase of the excess oxygen
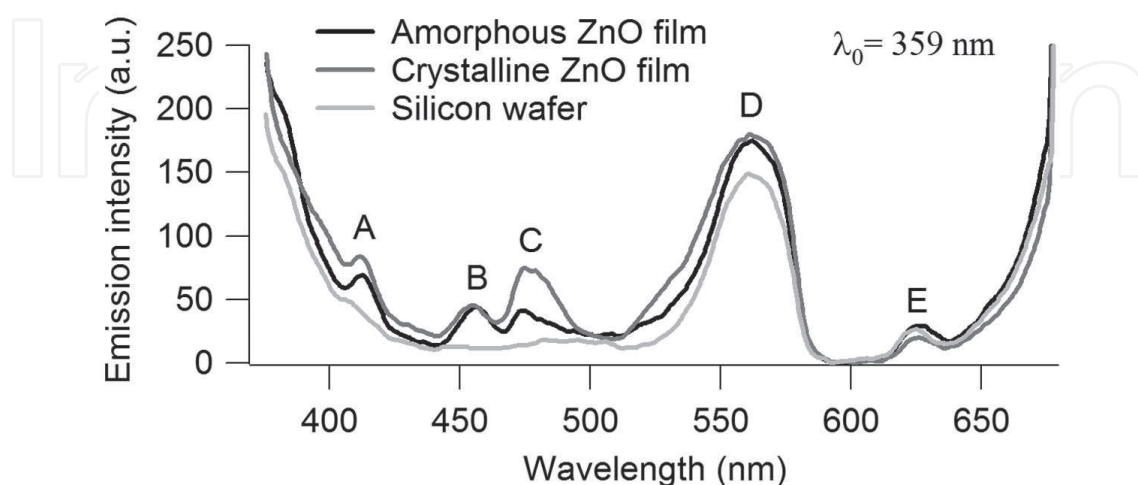
Figure 8. Emission spectra of crystalline ZnO film (intense gray solid line), amorphous ZnO film (black dotted line), and silicon wafer (gray solid line).

Film	Maximum emission peaks		
Amorphous	413 nm (3.0 eV)	456 nm (2.7 eV)	475 nm (2.6 eV)
Crystalline	411 nm (3.0 eV)	455 nm (2.7 eV)	474 nm (2.6 eV)

Table 3. Maximum emission peaks from amorphous and crystalline ZnO films.

concentrations and oxygen interstitials [4]. A slight blue shift means an improvement in the emissions [33, 34].

The violet emission peak located at 413–411 nm is due to the electron transition from the conduction band edge to the Zn vacancy level [33]. **Figure 9** shows the calculated energy levels of the intrinsic defects in ZnO applying full-potential linear muffin-tin orbital method [35]. Since it can be observed, the energy of the transition from conduction band to the Zn vacancies (V_{Zn}) corresponds to a violet emission with an energy of 3.0 eV [36]. Probably, these vacancies are on the grain boundaries. Other defects are the oxygen interstitial and oxygen antisite (O_{Zn}) which also favor the formation of an oxygen-rich environment.

The blue emission band observed at 456–455 nm (2.7 eV) could be produced by the electron transition from the shallow donor level of oxygen vacancies [28] and zinc interstitials [37, 38] to the valence band. Oba et al. report that the oxygen vacancies and zinc interstitials possess formation energies [37–39]. Oxygen vacancies produce two defect donor levels: One is the deep donor level located at 1.3–1.6 eV below the conductor band [40, 41] and the other is the shallow donor level below the conductor band in the range of 0.3–0.5 eV [41]. Valverde et al. calculated photon energy of the 2.7 eV from blue emission, which coincides with the value of 2.8 eV for the energy interval from the shallow donor level to the top of the valence band. Also, the energy level of zinc interstitials was located at 2.9 eV above the valence band for the samples with an energy gap of 3.36 eV [40]. For ZnO film with an energy gap of 3.4 eV, the energy level of zinc interstitials was around 2.72 eV above the valence band, which corresponds to a blue emission with a photon energy of the 2.7 eV (**Figure 9**). Finally, the blue band emission located at 475–474 nm (2.6 eV) from ZnO has been reported, but its exact origin has not been explained yet.
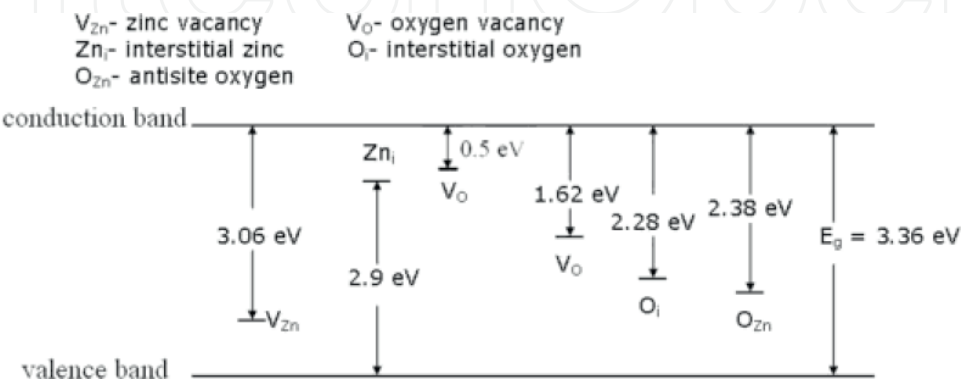
Figure 9. Schematic representation of calculated defect level in ZnO nanostructures.

Zinc oxide has been an important industrial material for centuries and is currently the subject of considerable new interest. As luminescent material, it has potential technological applications. Its different emissions as near ultraviolet, red, green, and blue can be substantially altered by the kind of substrate where the film is deposited and the synthesis method. Without a doubt, the sol-gel method is a friendly route to obtain uniform and stable zinc oxide films with high optical quality. Up to this time, the assignment of the emission bands is similar for different synthesis and substrates.

Acknowledgements

Author details

Guadalupe Valverde Aguilar*, Mónica R. Jaime Fonseca, Ángeles Mantilla Ramírez and Antonio G. Juárez Gracia

*Address all correspondence to: mvalverde@ipn.mx

CICATA-Legaria, Instituto Politécnico Nacional, Cd. de México, México

References

[1] Marci G, Augugliaro V, López-Munoz MJ, Martin C, Palmisano L, Rives V. Preparation, characterization and photocatalytic activity og polycrystalline ZnO/TiO_2 systems. Journal of Physical Chemistry B. 2001;**105**(5):1026-1032. DOI: 10.1021/jp003173j

[2] Hsu CC, Wu NL. Synthesis and photocatalytic activity of ZnO/ZnO_2 composite. Journal of Phochemistry and Photobiology A: Chemistry. 2005;**172**(3):269-274. DOI: 10.1016/j.jphotochem.2004.12.014

[3] Zhang DK, Liu YC, Liu YL, Yang H. The electrical properties and the interfaces of CuO/ZnO/ITO p-i-n heterojunction. Physica B: Condensed Matter. 2004;**351**(1):178-183. DOI: 10.1016/j.physb.2004.06.003

[4] Djurišić AB, Leung YH, Tam KH, Hsu YF, Ding L, Ge WK, Zhong YC, Wong KS, Chan WK, Tam HL, Cheah KW, Kwok WM, Phillips DL. Defect emissions in ZnO nanostructures. Nanotechnology. 2007;**18**(9):095702. DOI: 10.1088/0957-4484/18/9/095702

[5] Valverde-Aguilar G, García-Macedo JA, Juárez-Arenas R. Photoconductivity on nanocrystalline $ZnO-TiO_2$ thin films obtained by sol-gel. Proceedings of SPIE. 2008;**7041**:1-9. DOI: 10.1117/12.795461

[6]   García-Macedo J, Valverde-Aguilar G, Gómez RW, Pérez- Mazariego JL, Marquina V. Optical properties of nanostructured sol-gel thin films doped with Fe_2O_3 and the study of their ferromagnetic properties by Mössbauer spectroscopy. Journal of Nanoscience and Nanotechnology. 2008;**8**(12):6491-6496. DOI: 10.1166/jnn.2008.019

[7]   Yamamoto A, Atsuta S, Kanemitsu Y. Fabrication of ZnO nanocrystals dispersed in glass films for low-temperature optical studies. Physica E. 2005;**26**(1-4):96-99. DOI: 10.1016/j. physe.2004.08.031

[8]   Pan Z, Zhang P, Tian X, Cheng G, Xie Y, Zhang H, Zeng X, Xiao C, Hu G, Wei Z. Properties of fluorine and tin co-doped ZnO thin films deposited by sol-gel method. Journal of Alloys Compounds. 2013;**576**:31-37. DOI: 10.1016/j.jallcom.2013.04.132

[9]   Mohanta SK, Lee SH, Kong BH, Cho HK. Behavior of ultraviolet emission from nano-crystalline embedded ZnO film synthesized by solution-based route. Journal of Crystal Growth. 2009;**311**(6): 1539-1544. DOI: 10.1016/j.jcrysgro.2009.01.104

[10] Tai W-P, Oh J-H. Humidity sensing behaviors of nanocrystalline Al-doped ZnO thin films prepared by sol-gel process. Journal of Materials Science: Materials in electronics. 2002;**13**(7): 391-394. DOI: 10.1023/A:1016084309094

[11] Brinker CJ, Scherer GW. Sol-Gel Science: The Physics and Chemistry of Sol–Gel Processing. San Diego, CA: Academic Press; 1990. ISBN: 978-008057103-4

[12] Hench LL, West JK. The Sol-Gel Process. Chemical Reviews. 1990;**90**(1):33-72. DOI: 10.1021/cr00099a003

[13] Dave BC, Dunn B, Valentine JS, Zink JI. Sol-Gel Encapsulation methods for biosensors. Analytical Chemistry. 1994;**66**(22): 1120A-1127A. DOI: 10.1021/ac00094a001

[14] Dunn B, Zink JI. Optical properties of sol-gel glasses doped with organic molecules. Journal of Materials Chemistry. 1991;**1**(6): 903-913. DOI: 10.1039/JM9910100903

[15] Kachurin GA, Tyschenko IE, Zhuravlev KS, Pazdnikov NA, Volodin VA, Gutakovsky AK, Leier AF, Skorupa W, Yankov RA. Visible and near infrared luminescence from silicon nanostructures formed by ion implantation and pulse annealing. Nuclear Instruments and Methods in Physics Research B: Beam Interactions with Materials and Atoms. 1997;**122**(3):571-574. DOI: 10.1016/S0168-583X(96)00764-1

[16] Kayakuma Y. Quantum size effects of interacting electrons and holes in semiconductor microcrystals with spherical shape. Physical Review B. 1988;**38**(14-15):9797-9805. DOI: http://dx.doi.org/10.1103/PhysRevB.38.9797

[17] Urbieta A, Fernandez P, Hardalov Ch, Piqueras J, Sekiquchi T. Cathodoluminescence and scanning tunneling spectroscopy of ZnO single crystals. Materials Science and Engineering: B. 2002;**91-92**: 345-348. DOI: 10.1016/S0921-5107(01)01062-5

[18] Xiong G, Wilkinson J, Lyles J, Ucer KB, Williams RT. Luminescence and stimulated emis-sion in zinc oxide nanoparticles, films, and crystals. Radiation Effects and Defects in Solids. 2003;**158**(1-6):83-88. DOI: 10.1080/1042015022000037607

[19] Zu P, Tang ZK, Wong GKL, Kawasaki M, Ohtomo A, Koinuma H, Segawa Y. Ultraviolet spontaneous and stimulated emissions from ZnO microcrystallite thin films at room temperature. Solid State Communications. 1997;103(8): 459-463. DOI:10.1016/S0038-1098(97)00216-0

[20] Li BS, Liu YC, Zhi ZZ, Shen DZ, Lu YM, Zhang JY, Fan XW. The photoluminescence of ZnO thin films grown on Si (100) substrate by plasma-enhanced chemical vapor deposition. Journal of Crystal Growth. 2002;240(3-4):479-483. DOI: 10.1016/S0038-1098(97)00216-0

[21] van Dijken A, Meulenkamp EA, Vanmaekkelberh D, Meijerink A. The luminescence of nanocrystalline ZnO particles: the mechanism of the ultraviolet and visible emission. Journal of Luminescence. 2000;87-89:454-456. DOI: 10.1016/S0022-2313(99)00482-2

[22] Liu YX, Liu YC, Shen DZ, Zhong GZ, Fan XW, Kong XG, Mu R, Henderson DO. The structure and photoluminescence of ZnO films prepared by post-thermal annealing zinc-implanted silica. Journal of Crystal Growth. 2002;240:152-156. DOI: 10.1016/S0022-0248(02)00843-6

[23] Hirai T, Harada Y, Hasimoto S, Edamatsu K, Itoh T. Lifetimes of excitons in ZnO fine particles dispersed in alkali halide crystals. Journal of Luminescence. 2001;94-95:261-265. DOI: 10.1016/S0022-2313(01)00290-3

[24] Valverde-Aguilar G, Manríquez Zepeda JL. Photoluminescence and Photoconductivity studies on amorphous and crystalline ZnO thin films obtained by sol-gel method. Applied Physics A. 2015;118(4):1305-1313. DOI: 10.1007/s00339-014-8836-y

[25] Valle GG, Hammer P, Pulcinelli SH, Santilli CV. Transparent and conductive ZnO:Al thin films prepared by sol-gel dip-coating. Journal of the European Ceramic Society. 2004;24(6):1009-1013. DOI: 10.1016/S0955-2219(03)00597-1

[26] Wang Y-de, Zhang S, Wu X-hui. Green Light Luminescence from ZnO/Dodecylamine Mesolamellar Nanocomposites synthesized by Self-Assembly. European Journal of Inorganic Chemistry. 2005;2005(4):727-731. DOI: 10.1002/ejic.200400450

[27] Pal B, Sharon M. Enhanced photocatalytic activity of highly porous ZnO thin films prepared by sol-gel process. Materials Chemistry and Physics. 2002;76(1):82-87. DOI: 10.1016/S0254-0584(01)00514-4

[28] Wang Z, Zhang H, Wang Z, Zhang L, Yuan J. Structure and strong ultraviolet emission characteristics of amorphous ZnO films grown by electrophoretic deposition. Journal of Materials Research. 2003;18(1):151-155. DOI: http://dx.doi.org/10.1557/JMR.2003.0021

[29] Tokumoto MS, Briois V, Santilli CV, Pulcinelli SH. Preparation of ZnO Nanoparticles: Structural Study of the Molecular Precursor. Journal of Sol-gel Science and Technology 2003;26(1):547-551. DOI: 10.1023/A:1020711702332

[30] Kamalasanan MN, Chandra S. Sol-Gel synthesis of ZnO thin films. Thin Solid Films. 1996;288(1-2):112-115. DOI:10.1016/S0040-6090(96)08864-5

[31] Jeong S-H, Kim B-S, Lee B-T. Photoluminescence dependence of ZnO films grown on Si(100) by radio-frequency magnetron sputtering on the growth ambient. Applied Physics Letters. 2003;**82**(16):2625-2627. DOI: 10.1063/1.1568543

[32] Nadarajah K, Chee CY, Tan CY. Influence of annealing on properties of spray deposited ZnO thin films. Journal of Nanomaterials. 2013;**2013**:Article ID 146382, 8 pages. DOI: 10.1155/2013/146382

[33] Chen S, Zhao Z, Tang BZ, Kwok HS. Growth methods, enhanced photoluminescence, high hydrophobicity and light scattering of 4, 4'-bis(1, 2, 2-triphenylvinyl)biphenyl nanowires. Organic Electronics. 2012;**13**(10):1996-2002. DOI:10.1016/j.orgel.2012.06.014

[34] Sun YM. Study on the electronic structure of ZnO and its defects by using FP-LMTO method [thesis]. University of Science and Technology of China; 2000.

[35] Kale RB, Hsu Y-J, Lin Y-F, Lu S-Y. Synthesis of stoichiometric flowerlike ZnO nanorods with hundred percent morphological yield. Solid State Communications. 2007;**142**(5):302-305. DOI: 10.1016/j.ssc.2007.02.022

[36] Zhang DH, Xue ZY, Wang QP. The mechanisms of blue emission from ZnO films deposited on glass substrate by r.f. magnetron sputtering. Journal of Physics D: Applied Physics. 2002;**35**(21): 2837-2840. DOI: 10.1088/0022-3727/35/21/321

[37] Oba F, Nishitani SR, Isotani S, Adachi H, Tanaka I. Energetics of native defects in ZnO. Journal of Applied Physics. 2001;**90**(2):824-828. DOI:10.1063/1.1380994

[38] Kumar V, Kumar, V, Som S, Yousif A, Singh N, Ntwaeaborwa OM, Kapoor A, Swart HC. Effect of annealing on the structur, morphological and photoluminescence properties of ZnO thin films prepared by spin coating. Journal of Colloid and Interface Science. 2014;**428**:8-15. http://dx.doi.org/10.1016/j.jcis.2014.04.035

[39] Lin BX, Fu ZX, Jia YB. Green luminescent center in undoped zinc oxide films deposited on silicon substrates. Applied Physics Letters. 2001;**79**(7):943-945. DOI: 10.1063/1.1394173

[40] Xu PS, Sun YM, Shi CS, Xu FQ, Pan HB. Native Point Defect States in ZnO. Chinese Physics Letters. 2001;**18**(9):1252-1253. DOI: 10.1088/0256-307X/18/9/331

[41] Fu ZX, Guo CX, Lin BX, Liao GH. Cathodoluminescence of ZnO Films. Chinese Physics Letters. 1998;**15**(6):457-459. DOI: 10.1088/0256-307X/15/6/025